

# Structural Determination and Toll-like Receptor 2-dependent Proinflammatory Activity of Dimycolyl-diarabino-glycerol from *Mycobacterium marinum*<sup>\*S</sup>

Received for publication, May 3, 2012, and in revised form, July 11, 2012. Published, JBC Papers in Press, July 13, 2012, DOI 10.1074/jbc.M112.378083

Elisabeth Elass-Rochard<sup>‡S1</sup>, Yoann Rombouts<sup>‡S</sup>, Bernadette Coddeville<sup>‡S</sup>, Emmanuel Maes<sup>‡S</sup>, Renaud Blervaque<sup>¶</sup>, David Hot<sup>¶</sup>, Laurent Kremer<sup>||\*\*</sup>, and Yann Guérardel<sup>‡S</sup>

From the <sup>‡</sup>Université Lille Nord de France, Université Lille1, Unité de Glycobiologie Structurale et Fonctionnelle, UGSF, IFR 147 and <sup>S</sup>CNRS, UMR 8576, F-59650 Villeneuve d'Ascq, France, <sup>¶</sup>Laboratoire Transcriptomique et Génomique Appliquée, Centre d'Infection et d'Immunité de Lille-Institut Pasteur de Lille, U1019, UMR 8204, 1 rue du professeur Calmette, F-59019 Lille, France, and <sup>||</sup>Laboratoire de Dynamique des Interactions Membranaires Normales et Pathologiques (DIMNP), Université de Montpellier II et I, CNRS UMR 5235, case 107, and <sup>\*\*</sup>INSERM, DIMNP, Place Eugène Bataillon, 34095 Montpellier Cedex 05, France

**Background:** Cell wall-associated glycolipids contribute to the pathogenesis of mycobacterial infections.

**Results:** The structure of dimycolyl-diarabino-glycerol (DMAG) from *Mycobacterium marinum* was determined, and this glycolipid stimulated a potent TLR-2-dependent proinflammatory response in macrophages.

**Conclusion:** These findings strongly suggest that DMAG modulates the host immune system.

**Significance:** The biological relevance of DMAG activity in immunopathogenesis of mycobacterial infection needs to be addressed.

Although it was identified in the cell wall of several pathogenic mycobacteria, the biological properties of dimycolyl-diarabino-glycerol have not been documented yet. In this study an apolar glycolipid, presumably corresponding to dimycolyl-diarabino-glycerol, was purified from *Mycobacterium marinum* and subsequently identified as a 5-*O*-mycolyl- $\beta$ -Araf-(1 $\rightarrow$ 2)-5-*O*-mycolyl- $\alpha$ -Araf-(1 $\rightarrow$ 1')-glycerol (designated Mma\_DMAG) using a combination of nuclear magnetic resonance spectroscopy and mass spectrometry analyses. Lipid composition analysis revealed that mycolic acids were dominated by oxygenated mycolates over  $\alpha$ -mycolates and devoid of *trans*-cyclopropane functions. Highly purified Mma\_DMAG was used to demonstrate its immunomodulatory activity. Mma\_DMAG was found to induce the secretion of proinflammatory cytokines (TNF- $\alpha$ , IL-8, IL-1 $\beta$ ) in human macrophage THP-1 cells and to trigger the expression of ICAM-1 and CD40 cell surface antigens. This activation mechanism was dependent on TLR2, but not on TLR4, as demonstrated by (i) the use of neutralizing anti-TLR2 and -TLR4 antibodies and by (ii) the detection of secreted alkaline phosphatase in HEK293 cells co-transfected with the human *TLR2* and secreted embryonic alkaline phosphatase reporter genes. In addition, transcriptomic analyses indicated that various genes encoding proinflammatory factors were up-regulated after exposure of THP-1 cells to Mma\_DMAG. Importantly, a wealth of other regulated genes related to immune and inflammatory responses, including chemokines/cytokines and their respective receptors, adhesion molecules, and metalloproteinases, were found to be modulated by Mma\_DMAG. Overall, this study suggests that DMAG may be an active cell wall glyco-

conjugate driving host-pathogen interactions and participating in the immunopathogenesis of mycobacterial infections.

Tuberculosis, caused by *Mycobacterium tuberculosis*, remains a major threat to worldwide health. The incapacity to eradicate this disease is due in part to the unique mycobacterial cell envelope that plays a crucial role in widespread antibiotic resistance and pathogenesis (1). Phylogenetic studies have shown that *Mycobacterium marinum* (*Mma*)<sup>2</sup> is closely related to *Mycobacterium tuberculosis* (2). This species causes systemic tuberculosis-like in fish and other ectotherms involving persistent growth within macrophages (3) and induces “fish tank disease” in humans (4), characterized by the induction of a granulomatous infection. The systemic granulomatous diseases caused by *Mma* in fish share many histological traits with human tuberculosis including the granuloma formation and the ability of *Mma* to persist in a latent state without causing disease (5). Moreover, *M. tuberculosis* and *Mma* share many virulence factors, and in general, *M. tuberculosis* virulence genes can complement orthologous-mutated *Mma* genes (6, 7). Importantly, *Mma* infection of its natural hosts, especially zebrafish, has recently emerged as a useful model to study tuberculosis (5, 6, 8–13). This well-established embryology model is turning into a prominent model for immunological studies and particularly to decipher the interactions between *Mma* in its natural host as well as to address the contribution of

\* This work was supported by National Research Agency Grant ANR-05-MIIM-025 (to Y. G. and L. K.) and a grant from the Ministère de l'Enseignement Supérieur (to Y. R.).

<sup>S</sup> This article contains supplemental Tables S1 and S2.

<sup>1</sup> To whom correspondence should be addressed. Tel.: 33-3-20-43-41-42; E-mail: elisabeth.lass@univ-lille1.fr.

<sup>2</sup> The abbreviations used are: *Mma*, *M. marinum*; DMAG, dimycolyl-diarabino-glycerol; LM, lipomannan; TDM, trehalose-dimycolate; GMM, glucosylmonomycolate; GroMM, glycerol monomycolate; mAGP, mycolyl-arabinogalactan-peptidoglycan; TLR, toll-like-receptor; ICAM-1, intercellular adhesion molecule 1; SEAP, secreted embryonic alkaline phosphatase; TOCSY, two-dimensional total correlation spectroscopy; HSQC, heteronuclear single quantum correlation; LOS, lipooligosaccharide; PE, phosphatidylethanolamine.

the innate immune system in the infection process (14). However, to gain insight into the biological significance of cell envelope-associated molecules in the immunopathology of *Mma* infection in zebrafish, it is important to better define the structural diversity of the immunostimulatory *Mma* components.

The mycobacterial cell wall comprises long-chain fatty acids ( $C_{70}$ - $C_{90}$ ), the mycolic acids, that can be associated to extractable glycolipids or linked to the arabinogalactan-peptidoglycan insoluble backbone to form mycolyl-arabinogalactan-peptidoglycan (mAGP). According to the presence of various chemical functions on the meromycolic chain, mycolic acids are generally subdivided into  $\alpha$ -, keto-, and methoxy-mycolates (15). mAGP serves as an anchoring matrix for a vast array of (glyco) lipids that play a critical role in the modulation of the host immune system (16–19). Among them, mycolylated glycolipids such as trehalose-dimycolates (TDM), glucose-monomycolate (GMM), or glycerol monomycolate (GroMM) have been extensively scrutinized with respect to their structures and immunological properties. TDM for instance is regarded as one of the most bioactive and granulomatogenic cell wall glycolipid, exerting a potent adjuvant effect and playing a key role in mycobacterial virulence, mainly by stimulating both the innate and adaptive immunity (16, 20–22). After exposure to TDM, macrophages produce a broad panel of proinflammatory cytokines (TNF- $\alpha$ , IL1- $\beta$ , IL-12) and chemokines (IL-8, MCP-1, and MIP-1 $\alpha$ ) that are essential for granuloma formation in mice and guinea pigs (21–24). Macrophage surface C-type lectin Mincle or Toll-like receptor 2 (TLR2), in combination with MARCO scavenger receptor/CD14 complex, have been demonstrated to interact with TDM (25–28). The two mycolic acids on TDM reflect the mycolic acid composition of the mycobacterial strain from which the TDM is isolated. As such, the chemical structure of TDM varies substantially between strains because the mycolic acid composition differs according to mycobacterial strains. These strain differences provide a natural source of chemically distinct TDM mixtures that can be tested for biological activity. Interestingly, it was demonstrated that mycolic acid composition of TDM influences the inflammatory activity of this glycolipid. Therefore, TDM activities largely depend on the chemical nature of mycolates attached to the trehalose backbone (29, 30).

Two decades ago, another mycolic acid-containing glycolipid, designated dimycolyl-diarabino-glycerol (DMAG), was found in the *Mycobacterium avium-intracellulare* complex and in *Mycobacterium kansasii* (31, 32). Recently, this amphiphathic hydrophobic glycolipid was identified in the cell wall of other slow-growing mycobacterial species including *M. tuberculosis*, *Mycobacterium bovis* BCG, *Mycobacterium scrofulaceum*, and *Mma* (33). Structural analyses demonstrated that DMAG from *M. bovis* BCG is analogous to the terminal portion of mycolyl-arabinogalactan-peptidoglycan, consisting in 5-*O*-mycolyl- $\beta$ -Araf-(1 $\rightarrow$ 2)-5-*O*-mycolyl- $\alpha$ -Araf-(1 $\rightarrow$ 1)-Gro (DMAG) (33). Moreover, exposure to anti-tubercular drugs (thiacetazone, ethambutol) known to interfere with the mAGP and mycolate biosynthesis altered DMAG production in both *Mma* and *M. bovis* BCG, leading to the hypothesis of a metabolic relationship between DMAG and mAGP (33). In addition, the presence of anti-DMAG antibodies in patients infected with *M. avium*

strongly suggested that DMAG is an immunogenic compound produced (or released from the cell wall) during infection (34). However, despite the high structural analogy between DMAG and other mycolylated glycolipids, no investigation has been conducted yet regarding the eventual immunomodulatory properties of DMAG and whether this glycoconjugate interacts with the host immune receptors. The relevance of this glycolipid during mycobacterial pathogenesis remains to be fully addressed.

This study was, therefore, undertaken as a first step to decipher DMAG biological properties by focusing on its capacity to modulate the macrophage immune response and the molecular basis for macrophage recognition of DMAG. To extend our previous studies on the structural variability of *Mma* glycolipids and to gain new insight with respect to their biological functions, we have performed the detailed structural analysis of a family of mycolylated arabino-glycero lipids from *Mma*, which allowed us to assign three related molecules. The major member of this family, *Mma*\_DMAG, was used to investigate the ability of the arabinosylated glycolipids to induce both proinflammatory cytokine secretion and expression of cell surface antigens in the human macrophage-like differentiated THP-1 cell line via a Toll-like receptor-dependent mechanism. Furthermore, these results were not only confirmed but also extended at a whole transcriptomic level in THP-1 cells exposed to *Mma*\_DMAG. These findings provide the first report on the immunomodulatory activity of this apolar glycoconjugate.

## EXPERIMENTAL PROCEDURES

**Mycobacteria and Growth Culture Conditions**—*Mma* strain 7 (E7) was originally isolated from butterfly fish (35). It was grown at 30 °C in Sauton's medium or on plates containing Middlebrook 7H10 agar supplemented with 10% oleic acid, albumin, dextrose, and catalase enrichment.

***Mma*\_DMAG Extraction and Purification**—Apolar lipids containing DMAG were extracted from 40 g of wet cells (around 10 liters of culture) of *Mma* according to established procedures (36). *Mma*\_DMAG was then purified by two successive rounds of absorption chromatography, as reported earlier (33). Briefly, the crude apolar extract was dissolved in chloroform and fractionated by silica gel column flash chromatography. The column was eluted with chloroform and chloroform/methanol with increasing volumes of methanol (1–50%). Purification of the *Mma*\_DMAG was monitored by one-dimensional high performance TLC (Merck) using chloroform/methanol (96:4, v/v) or chloroform/methanol (90:10, v/v). Glycolipids were visualized by spraying plates with orcinol/sulfuric acid reagent followed by charring at 120 °C. *Mma*\_DMAG fractions containing 5–7% of methanol were pooled and applied on a Florisil® column chromatography (Acros Organics). Elution was performed with chloroform followed by chloroform/methanol with increasing volumes of methanol (2–20%). Purification monitored by high performance TLC after spraying with orcinol/sulfuric acid. *Mma*\_DMAG was eluted in fractions containing 7% of methanol and *Mma*\_DMAG-containing fractions were pooled for structural analyses. Finally, the yield for the DMAG was about 770  $\mu$ g/liter of culture.

## Proinflammatory Activity of Mycobacterial DMAG

**Purification of Lipomannan**—Lipomannan (LM), a known proinflammatory-inducing factor, was purified from *Mma* using procedures reported previously (37).

**Endotoxin Levels**—Potential contamination by endotoxin in *Mma*\_DMAG and LM samples was evaluated using the *Limulus* amoebocyte lysate assay kit (QCL1000; Cambrex). No endotoxin was detected in *Mma*\_DMAG sample, whereas the LM preparation contained insignificant amounts of endotoxin (<50 pg/10 µg of LM).

**Extraction of Mycolic Acids from DMAG**—Extraction of mycolic acid methyl esters was carried out as described previously (38, 39). Briefly, purified DMAG were subjected to alkaline hydrolysis in 1 ml of 15% tetrabutylammonium hydroxide at 100 °C overnight. After cooling, free mycolic acids were methyl-esterified by the additions of 2 ml of dichloromethane, 150 µl of iodomethane, and 1 ml of water. The mixture was sonicated and then centrifuged at 3500 rpm for 10 min. The aqueous phase was discarded, and the dichloromethane phase containing mycolic acid methyl esters was washed three times with 2 ml of water. Finally, the organic phase was evaporated under a stream of nitrogen, and the sample was diluted in chloroform before mass spectrometry analysis.

**Matrix-assisted Laser Desorption Ionization–Mass Spectrometry (MALDI-MS) Analysis**—The molecular masses of glycolipids were measured by MALDI-TOF on a Voyager Elite reflectron mass spectrometer (PerSeptive Biosystems, Framingham, MA) equipped with a 337-nm UV laser. Samples were prepared by mixing 5 µl of glycolipid solution in chloroform and 5 µl of 2,5-dihydroxybenzoic acid matrix solution (10 mg/ml dissolved in chloroform/methanol (1/1, v/v)). The mixtures (2 µl) were then spotted on the target.

**NMR Analysis**—NMR experiments were recorded at 300 K on a Bruker Avance 400 spectrometer equipped with a 5-mm broad-band inverse probe, respectively. Before NMR spectroscopic analyses, *Mma*\_DMAG was repeatedly exchanged in CDCl<sub>3</sub>/CD<sub>3</sub>OD (2:1, v/v) (99.97% purity, Euriso-top, Saint-Aubin, France) with intermediate drying and finally dissolved in CDCl<sub>3</sub> and transferred to Shigemi (Allison Park, PA) tubes. Chemical shifts (ppm) were calibrated using the tetramethylsilane signal ( $\delta^1\text{H}/\delta^{13}\text{C}$  0.000 ppm) in CDCl<sub>3</sub> as an internal reference. The COSY, TOCSY, and <sup>13</sup>C HSQC experiments were performed using the Bruker standard sequences.

**Cell Culture Conditions**—Human pro-monocytic leukemia THP-1 cells (ECACC no. 88081201) were grown in RPMI 1640 supplemented with 10% FCS, 2 mM L-glutamine, and  $2 \times 10^{-5}$  M  $\beta$ -mercaptoethanol in a 5% CO<sub>2</sub>/air-humidified atmosphere at 37 °C. Differentiation into macrophage-like cells was induced with 50 nM 1,25-dihydroxyvitamin D3 for 72 h in RPMI 1640 supplemented with 10% FCS and 2 mM L-glutamine. Viability of the cells was checked by trypan blue dye exclusion and by flow cytometry (FACSCalibur flow cytometer) by using propidium iodide. HEK-Blue-hTLR2 cells and HEK-Blue-Null1 cells were purchased from InVivoGen (Toulouse, France) and maintained in growth medium supplemented with HEK-blue selection according to the manufacturer's instructions. HEK-Blue-hTLR2 cells were obtained by co-transfection of the hTLR2 and secreted embryonic alkaline phosphatase (SEAP) reporter genes into human embryonic kidney 293 (HEK293)

cells. The SEAP reporter gene was placed under the control of the IFN- $\beta$  minimal promoter fused to five NF- $\kappa$ B and AP-1 binding sites. HEK-Blue Null1 cells, the parental cell line of HEK-Blue-hTLR2, carry the SEAP reporter gene alone.

**Quantification of Cytokine Secretion by ELISA**—To investigate the effect of *Mma*\_DMAG on TNF- $\alpha$ , IL-8, and IL-1 $\beta$  secretion, differentiated THP-1 cells were seeded in 96-well plastic culture plates at a density of  $25 \times 10^4$  cells/well in RPMI 1640 medium supplemented with 2% FCS and L-glutamine. Because *Mma*\_DMAG was insoluble in aqueous medium, it was resuspended in hexane at the indicated concentrations and coated on plates. Wells were subsequently dried at 37 °C to ensure complete solvent evaporation before cell addition. Control wells were layered with solvent without glycolipids. LM purified from *Mma*, dissolved in apyrogen water, and sonicated was used as a positive control. After 6 or 24 h of incubation, culture supernatants were collected and analyzed for the detection of TNF- $\alpha$ , IL-8, and IL-1 $\beta$  by sandwich ELISA according to the manufacturers' instructions (Ozyme S.A.). Cytokine concentrations were determined using standard curves obtained with recombinant human TNF- $\alpha$ , IL-1 $\beta$ , or IL-8. Statistical significance was determined using Student's *t* test (only values of  $p < 0.05$  were considered to be significant).

**Flow Cytometry Analysis**—The expression level of the cell surface markers was determined after stimulation of differentiated THP-1 cells (at a density of  $3.5 \times 10^5$  cells/well) with either *Mma*\_DMAG or LM in RPMI 1640 supplemented with 2% FCS and L-glutamine as previously reported (40). Control wells were layered without glycolipids. After 24 h of incubation, expression of human ICAM-1 (CD54) and CD40 was determined by flow cytometry. Briefly, 250,000 cells were incubated for 20 min at 4 °C with 20 µg/ml human IgG (Sigma), washed 3 times, and incubated for 40 min with 10 µl of PE-conjugated anti-ICAM-1 (CD54) or FITC-conjugated anti-CD40 mouse monoclonal IgG1 $\kappa$  antibodies (BD Biosciences) in PBS containing 0.04% NaN<sub>3</sub> and 0.05% BSA. Both PE- and FITC-conjugated mouse isotype control IgG (BD Biosciences) were used as negative controls. In all experiments, cells were washed twice. Data were monitored on a flow cytometer (FACSCalibur, BD Biosciences) and analyzed with the CellQuest software (Mountain View, CA). Cells were gated for forward- and side-angle light scatters, the fluorescence channels were set on a logarithmic scale, and the mean fluorescence intensity was determined.

**TLR Neutralization**—To address the participation of TLRs in the proinflammatory-inducing activity of *Mma*\_DMAG, differentiated macrophages were pretreated with 15 µg/ml neutralizing monoclonal against anti-TLR2 or anti-TLR4 for 30 min at 37 °C. Mouse IgG2a anti-TLR2 (clone TL2-1) was purchased from Biologend, whereas mouse IgG2 $\alpha$ κ was from eBiosciences. Cells were then stimulated with 20 µg/ml *Mma*\_DMAG for 6 or 24 h to allow TNF- $\alpha$  secretion or ICAM-1 expression, respectively. The corresponding isotype antibodies were used as negative controls. Supernatants were processed for TNF- $\alpha$  and IL-8 quantification by ELISA, whereas ICAM-1 expression was determined by flow cytometry, as described above. Statistical significance between antibody-pretreated cells and untreated cells was calculated by using Student's *t* test. Values with  $p < 0.05$  were considered significant.



**HEK-TLR2 Experiment**—HEK-Blue-hTLR2 that stably expresses the human TLR2 gene along with a NF- $\kappa$ B-inducible reporter system (secreted alkaline phosphatase) and the parental HEK-blue-Null1 cell line were seeded at  $5 \times 10^4$  cells/well in 96-wells plates and stimulated with either 20  $\mu$ g/ml Mma\_DMAG or 20 ng/ml lipopeptide Pam<sub>3</sub>Cys-SK<sub>4</sub> (Pam<sub>3</sub>CSK<sub>4</sub>, EMC Microcollections GmbH, Germany), a well known TLR2 agonist. Stimulation with a TLR2 ligand activates NF- $\kappa$ B and AP-1, which induce production of SEAP. After 20 h of incubation at 37 °C, SEAP activity was determined using the QUANTI-Blue detection kit by measuring the absorbance at 630 nm. Statistical significance of between the unstimulated and stimulated HEK-Blue-hTLR2 cells was determined using Student's *t* test, and only  $p < 0.05$  was considered significant.

**Microarrays Data Processing and Statistic Analyses**—Differentiated THP-1 cells ( $3 \times 10^6$ ) were incubated for 8 h either with medium alone or medium supplemented with 20  $\mu$ g/ml Mma\_DMAG. Total RNA was extracted from the cells using the Nucleospin RNA II kit (Macherey-Nagel, Düren), according to the manufacturer's instructions. RNA concentrations were determined using a NanoDrop 2000 spectrophotometer (NanoDrop Technologies), and RNA quality was assessed using Agilent RNA Nano 6000 LabChip kits and an Agilent 2100 Bioanalyzer (Agilent Technologies). All RNA samples had RNA integrity numbers of 9.7 or higher. A human ( $4 \times 44,000$ ) whole genome oligo DNA microarray chip (G4112F, Agilent Technologies) was used for global gene expression analysis. 2  $\mu$ g of total RNA was used in the Agilent Quick Amp Labeling kit according to the manufacturer's instructions. After purification using an RNeasy Mini Kit (Qiagen), cRNA yield and incorporation efficiency (specific activity) into the cRNA were determined using a NanoDrop 2000 (Thermo Scientific) spectrophotometer. For each sample, a total of 2  $\mu$ g of cRNA was fragmented and hybridized to the whole human genome oligo  $4 \times 44,000$  microarrays overnight at 65 °C. Slides were washed and treated with stabilizing and drying solution according to the manufacturer (Agilent Technologies). The array was scanned on a InnoScan 700 scanner (Innopsys) and further processed using Mapix 2.6.1 software. The resulting text files were uploaded into language R for analysis and analyzed using the LIMMA package (Linear Model for Microarray Data) (41, 42). A within-array normalization was performed using LOWESS (locally weighted linear regression) to correct for dye and spatial effects (43). Moderate *t*-statistic with empirical Bayes shrinkage of the standard errors (44) was then used to determine significantly modulated genes. Statistics were corrected for multiple testing using a false-discovery rate approach.

## RESULTS

**Structure of Mycobacterium marinum DMAG**—We have recently shown that several slow-growing mycobacterial species, including *M. bovis* BCG, *M. tuberculosis*, and *Mma* produce an apolar cell wall-associated glycolipid whose synthesis was altered by several anti-tubercular drugs inhibiting arabinogalactan or mycolic acid biosynthesis (33). Structural elucidation of this product in *M. bovis* BCG identified it as 5-O-mycolyl- $\beta$ -Araf-(1 $\rightarrow$ 2)-5-O-mycolyl- $\alpha$ -Araf-(1 $\rightarrow$ 1)-Gro, designated di-mycolyl di-arabino-glycerol (DMAG). To extend

these studies regarding the structural diversity of DMAG and to undertake structure/function relationship studies, we purified and determined the fine structure of DMAG in *Mma* strain 7. This natural strain, originally isolated from infected butterfly fish, has previously been reported to exhibit an altered lipooligosaccharide (LOS) profile compared with the standard *M* strain (45). As reported earlier, a glycolipid presumably corresponding to DMAG was purified from the apolar extract by adsorption chromatography on a silica gel column using a gradient of methanol in chloroform. This component yielded a major orcinol-reactive component with an  $R_f$  of 0.87 compared with 0.38 for TDM on TLC plates using chloroform/methanol (96:4; v/v) as a running solvent (Fig. 1A). In addition, two minor undefined glycolipids ( $R_f$  of 0.49 and 0.21, respectively) with chromatographic mobilities closer to TDM ( $R_f$  0.38) were also tentatively attributed to arabinose-containing glycolipids based on their distinctive intense blue color upon orcinol staining.

MALDI-TOF-MS analysis indicated that the DMAG from *Mma* (Mma\_DMAG) exhibited a heterogeneous molecular mass profile ranging from 2577 to 2947 Da, with the most abundant molecular species at 2790 and 2818 Da (Fig. 1B). MS analysis of the methyl-esterified lipid moiety released from Mma\_DMAG by alkaline hydrolysis revealed a heterogeneous pattern attributed to a mixture of alpha ( $\alpha$ ), keto (k), and methoxy-mycolates (m) with  $m/z$  values ranging from 1132 ( $\alpha$ C<sub>75</sub>) to 1346 (mC<sub>89</sub>) and dominated by two signals at  $m/z$  1274 and 1302 attributed to [M+Na]<sup>+</sup> adducts of C<sub>84</sub> and C<sub>86</sub> ketomycolates (Fig. 1C). Consistent with the prevalence of keto- and methoxy-mycolates over  $\alpha$ -mycolates, Mma\_DMAG subspecies were mainly found to be substituted by oxygenated mycolates. Indeed, based on the tentative presence of a Ara<sub>2</sub>Gro moiety, mycolate composition of major Mma\_DMAG signal clusters around  $m/z$  2790 and  $m/z$  2818 were assigned to DMAGs substituted by a mixture of keto- and methoxy-mycolates bearing totals of 166 and 168 carbons, respectively. The presence of oxygenated keto- and methoxy-mycolates was confirmed by <sup>1</sup>H NMR analysis of intact Mma\_DMAG (Fig. 1D). Furthermore, <sup>1</sup>H NMR analysis allowed us to detect the presence of *trans*- and *cis*-ethylene groups as well as *cis*-cyclopropane groups. The presence of *cis*-cyclopropane was established by the observation of CH<sub>2</sub> signals at  $\delta$  -0.33 and 0.57, whereas *trans*-cyclopropane functional groups could not be observed, in agreement with previous observations on total mycolic acids from *Mma* (46). The structure of the glycan moiety of Mma\_DMAG was next investigated by <sup>1</sup>H/<sup>1</sup>H COSY, TOCSY, and <sup>13</sup>C/<sup>1</sup>H HSQC NMR experiments, allowing us to attribute its individual <sup>13</sup>C/<sup>1</sup>H NMR parameters based on those previously assigned for *M. bovis* BCG DMAG (Fig. 2, Table 1) (33). As observed Fig. 2, two anomer signals were identified at <sup>13</sup>C/<sup>1</sup>H  $\delta$  4.99/106.0 and  $\delta$  5.02/101.5 ppm, thus confirming the presence of two different monosaccharides. Their spin systems determined by <sup>1</sup>H/<sup>1</sup>H NMR experiments typified them as 5-acylated  $\alpha$ -Araf and  $\beta$ -Araf residues, respectively (Fig. 2A). The deshielding of  $\alpha$ -Araf-C2 ( $\Delta\delta = +6.0$ ) compared with that of non-reducing terminal  $\alpha$ -Araf established that this residue was substituted in position C2 (Fig. 2B). Finally, the identification of a C1-substituted glycerol residue (Gro) confirmed the structure of Mma\_DMAG as 5-O-mycolyl- $\beta$ -Araf-(1 $\rightarrow$ 2)-5-O-mycolyl-

## Proinflammatory Activity of Mycobacterial DMAG

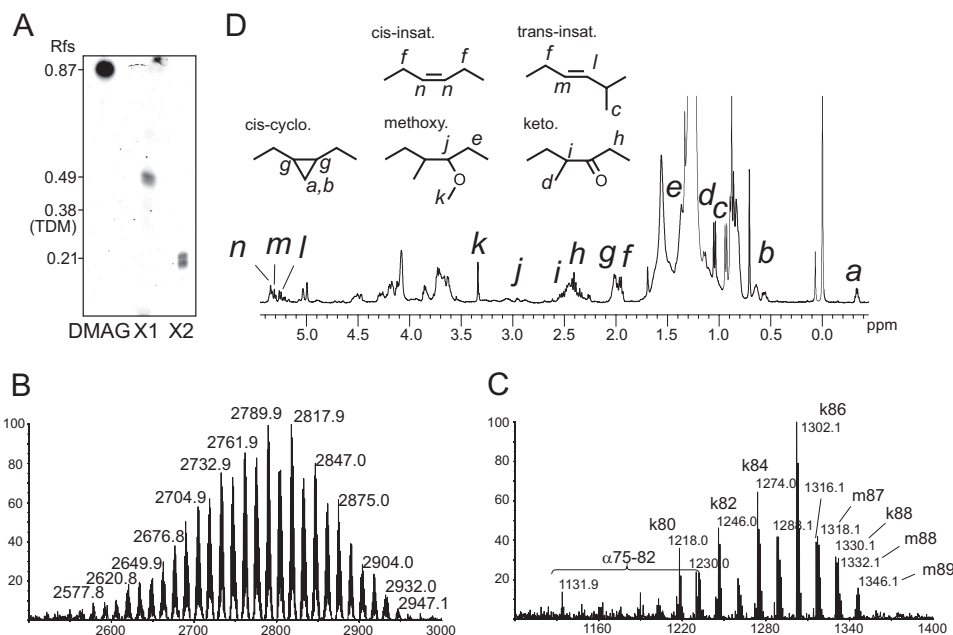


**FIGURE 1. Structural analysis of Mma\_DMAG.** A, a TLC profile of purified arabino-glycero lipids from *Mma* shows the major compound identified as di-mycolyl di-arabino-glycerol (Mma\_DMAG) and two minor related glycoconjugates identified as mono-mycolyl mono-arabino-glycerol (X1) and mono-mycolyl di-arabino-glycerol (X2).  $R_f$  are indicated in the *left margin*. MALDI-TOF-MS spectrum of intact Mma\_DMAG (B) and mycolic acid methyl esters (MAMEs) (C) derived from Mma\_DMAG show the presence of  $\alpha$ -, keto-, and methoxy-mycolic acids. D,  $^1\text{H}$  NMR spectrum of Mma\_DMAG; a to n indicate the relevant signals used for the identification of functional groups of mycolates.

$\alpha$ -Araf-(1 $\rightarrow$ 1)-Gro. Although not demonstrated in this study, the arabinose residues are believed to be in a D configuration based on the exclusive identification of D-Ara in all mycobacterial glycoconjugates so far and because of its postulated filiation with mAGP (33). Overall, this analysis indicates that DMAG from *Mma* is extremely similar to the one from *M. bovis* BCG, with the notable exception for its lipid moiety comprising a mixture of  $\alpha$ -, keto- and methoxy-mycolates in *Mma* instead of  $\alpha$ - and keto-mycolates only in *M. bovis* BCG. In addition, mycolates of Mma\_DMAG lack a *trans*-cyclopropane ring. Along with Mma\_DMAG, the partial structural analysis of the two minor arabinose-containing glycolipids (Fig. 1A) permitted their identification as 5-O-mycolyl- $\alpha$ -Araf-(1 $\rightarrow$ 1)-Gro and a mixture of  $\beta$ -Araf-(1 $\rightarrow$ 2)-5-O-mycolyl- $\alpha$ -Araf-(1 $\rightarrow$ 1)-Gro and 5-O-mycolyl- $\beta$ -Araf-(1 $\rightarrow$ 2)- $\alpha$ -Araf-(1 $\rightarrow$ 1)-Gro, respectively (data not shown). However, the limited amount of each of these compounds precluded further biological analyses.

**Proinflammatory Activity of Mma\_DMAG**—A plethora of reports demonstrated the immunomodulatory properties of cell wall-associated mycolylated glycolipids, which may represent key effectors in the induction of the host defense through the activation of macrophage and antigen presenting cells. Most studies have focused on TDM, GroMM, and GMM (22, 27, 47). Considering the structural similarity between these lipids with DMAG regarding their mycolic acid composition, we reasoned that the DMAG family of glycolipids may also participate to the modulation of the host immune response. To check this hypothesis, we first evaluated the ability of Mma\_DMAG to induce the secretion of proinflammatory cytokines in macrophages and to stimulate the expression of cell surface antigens.

TNF- $\alpha$  is a key mediator involved in the initiation and the maintenance of the granulomatous response (48, 49), whereas

IL-1 $\beta$  represents another important proinflammatory cytokine that contributes to anti-mycobacterial host defense mechanisms (50), whose production is induced by *M. tuberculosis* through different pathways involving TLR2/TLR6 and NOD2 receptors (51). IL-8 mediates the recruitment of neutrophils during mycobacterial infection (49). The capacity of Mma\_DMAG to trigger TNF- $\alpha$ , IL-1 $\beta$ , and IL-8 secretion was investigated on differentiated THP-1 cells, which have been extensively used to test the biological effects of mycobacterial glycolipids (52, 53). Mma\_DMAG was found to induce the release of TNF- $\alpha$  (Fig. 3A), IL-1 $\beta$  (Fig. 3B), and IL-8 (Fig. 3C) from differentiated cells. The optimal response regarding TNF- $\alpha$  secretion was achieved with 30  $\mu\text{g}/\text{ml}$  Mma\_DMAG. The level of cytokines induced by DMAG was about 18-fold higher for TNF- $\alpha$  and 30-fold higher for IL-1 $\beta$  compared with un-stimulated cells (medium alone). IL-8 production was also significantly increased (9-fold) in the presence of various concentrations of DMAG (Fig. 3C). LM purified from *Mma* was included as a positive control because it has been reported to exhibit a significant proinflammatory response (52–55). Mma\_DMAG exhibited, however a lower proinflammatory activity compared with LM (Fig. 3).

The interaction of ICAM-1 (CD54) with  $\alpha 1/\beta 2$  integrin (CD11a/CD18) leads to the activation and the proliferation of T cells, whereas the co-stimulatory protein CD40 is required for the activation of antigen presenting cells (56). To address whether DMAG stimulates the expression of macrophage cell surface markers, THP-1 macrophages were incubated with either LM or Mma\_DMAG and analyzed by flow cytometry using either PE-conjugated anti-ICAM-1 or FITC-conjugated anti-CD40 antibodies. As shown in Fig. 4, Mma\_DMAG induces the expression of both ICAM-1 and CD40 at the sur-

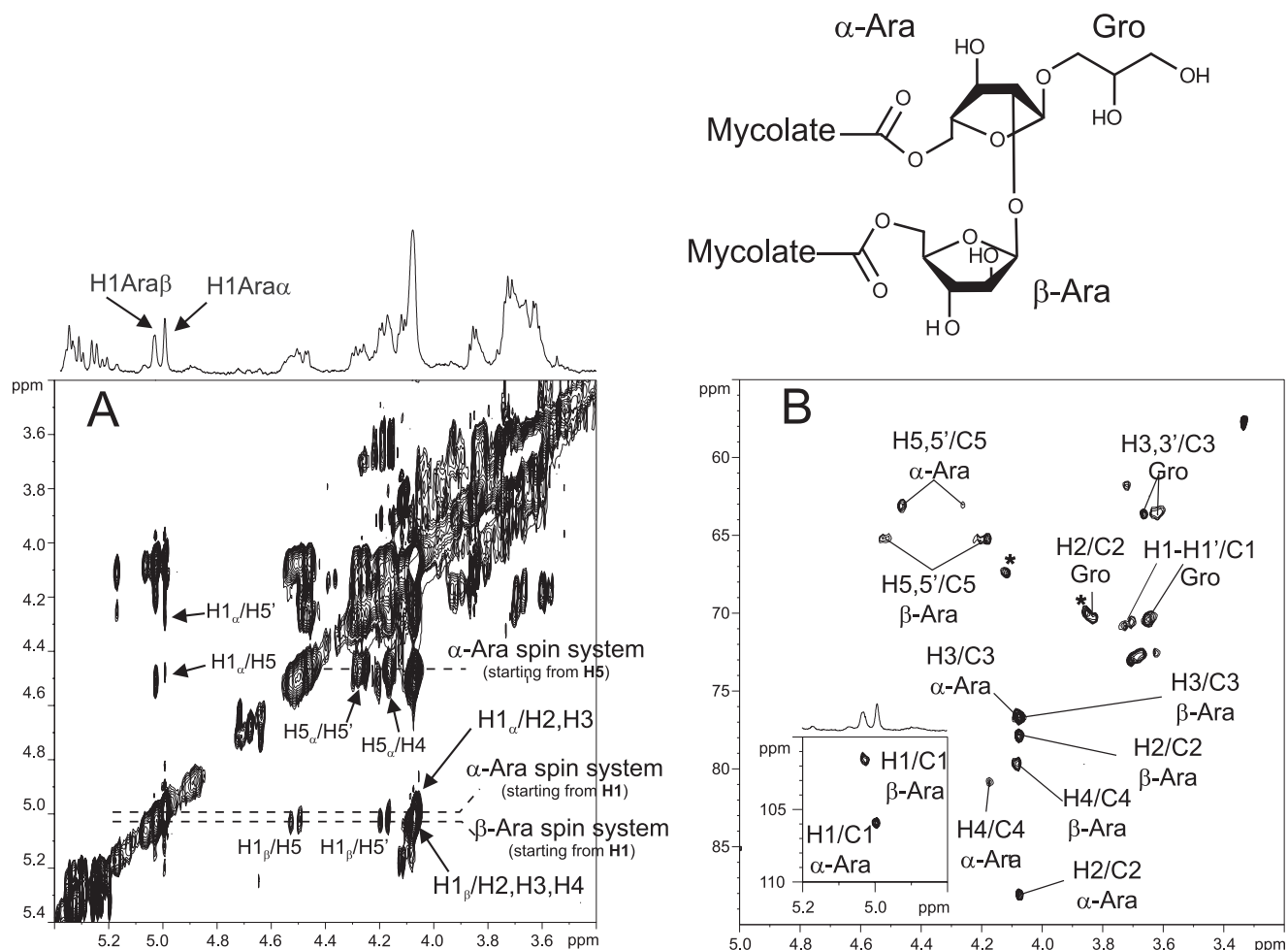


FIGURE 2. NMR analysis of the Mma\_DMAG glycan moiety.  $^1\text{H}/^1\text{H}$  TOCSY (A) and  $^{13}\text{C}, ^1\text{H}$  HSQC (B) NMR spectra of Mma\_DMAG permitted us to establish the structure of Mma\_DMAG as 5-O-mycolyl- $\beta$ -Araf-(1 $\rightarrow$ 2)-5-O-mycolyl- $\alpha$ -Araf-(1 $\rightarrow$ 1)-Gro.

TABLE 1

$^1\text{H}$  and  $^{13}\text{C}$  chemical shifts of 5-O-mycolyl- $\beta$ -Araf-(1 $\rightarrow$ 2)-5-O-mycolyl- $\alpha$ -Araf-(1 $\leftrightarrow$ 1')-Gro isolated from *M. marinum*

	H-1/C-1	H-2/C-2	H-3/C-3	H-4/C-4	H-5/C-5
$\beta$ -Araf	5.02/101.5	4.07/77.8	4.06/76.6	4.07/79.6	4.18, 4.52/65.2
$\alpha$ -Araf					

face of THP-1 cells, albeit to a lesser extent than LM. As expected, no significant fluorescence signal could be detected using isotype control antibodies.

Overall, these results indicate that, like other mycolic acid-containing glycolipids, DMAG is a biologically active molecule exhibiting potent proinflammatory activity and promoting macrophage activation, both being relevant to macrophage-lymphocyte interaction/recruitment and mycobacteria-induced immunopathogenesis.

**Macrophage Activation and Proinflammatory-induced Response by DMAG Are Dependent on TLR-2—TLRs** are known as key receptors for promoting the inflammatory immune response during microbial infection (55). TLR2 recognizes mycolic acid-containing lipids, such as TDM, in combination with other receptors (MARCO/CD14) present on macrophages (26). We next investigated the possible participation of TLR2 and/or TLR4 in the signaling pathway leading to THP-1 activation by Mma\_DMAG. Production of inflammatory cytokines/

chemokines by THP-1 cells as well as expression of cell surface receptors were followed by incubating cells with specific neutralizing TLR2 or TLR4 antibodies or their corresponding isotype control antibodies. As shown in Fig. 5A, pretreatment with anti-TLR2 antibodies, but not with anti-TLR4 or isotype control antibodies, was accompanied by a strong decrease in TNF- $\alpha$  and IL-8 secretion (with 71 and 62% inhibition in the presence of anti-TLR2 antibodies, respectively). Consistent with these findings, neutralization of TLR2 was also associated with a decrease in ICAM-1 cell surface expression induced by Mma\_DMAG (Fig. 5B). This effect was not observed when cells were pretreated with anti-TLR4 antibodies.

To further confirm the involvement of TLR2 in Mma\_DMAG-induced activity, HEK293-TLR2 cells co-transfected with both the human TLR2 gene and the SEAP-inducible reporter system were stimulated for 20 h with Mma\_DMAG. Lipopeptide Pam<sub>3</sub>CSK<sub>4</sub> and LM were included as positive TLR2 agonists. As judged by QUANTI-Blue detection, Mma\_DMAG exhibited dose-dependent NF- $\kappa$ B activation in HEK293-TLR2 cells (Fig. 5C). As expected, no induction was observed after stimulation of the parental HEK-Blue Null1 cells, thus demonstrating the specificity of the TLR2-dependent effect. It is noteworthy that the level of NF- $\kappa$ B activation



## Proinflammatory Activity of Mycobacterial DMAG

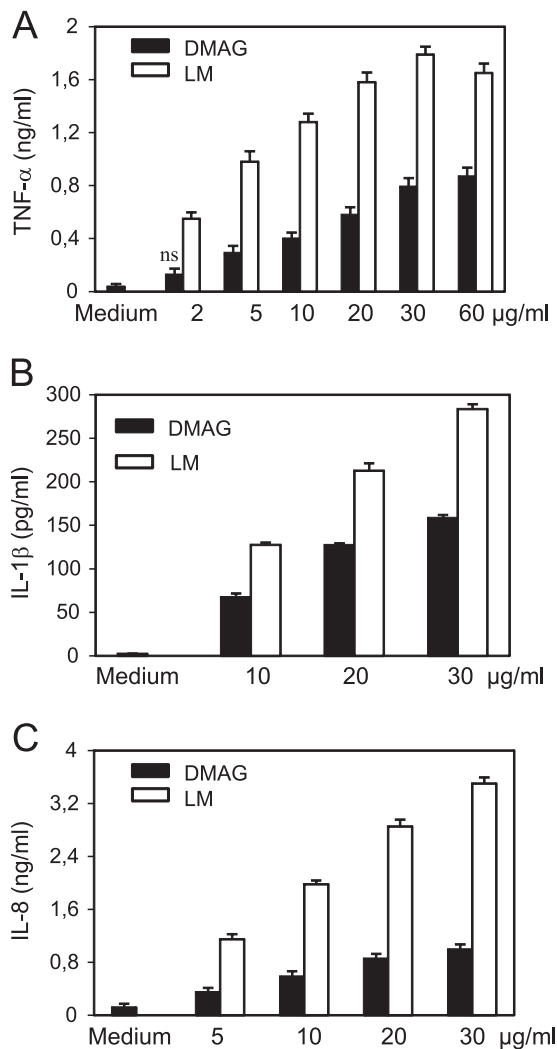


**FIGURE 3. Proinflammatory cytokines secretion by THP-1 macrophages stimulated with Mma\_DMAG.** Differentiated THP-1 cells were incubated with increasing concentrations of either Mma\_DMAG or LM from *Mma*. Culture supernatants were collected after 6 or 24 h and assayed by ELISA for TNF- $\alpha$  (A), IL-1 $\beta$  (B), and IL-8 (C) secretion. Data are expressed as the means  $\pm$  S.D. of triplicates and are representative from three independent experiments. Statistical analyses were performed by using Student's *t* test (*p* values were  $< 0.05$ ; *ns*, nonspecific *p*  $> 0.05$ ).

observed was lower with Mma\_DMAG than with LM or Pam<sub>3</sub>CSK<sub>4</sub>. Taken together, these results clearly reveal that Mma\_DMAG exerts its effects through ligation to TLR2, leading to the production of a prominent proinflammatory response and to macrophage activation.

**Transcriptomic Analyses of Mma\_DMAG-stimulated THP-1 Macrophages**—To gain insight toward the mechanisms by which DMAG interferes with the host immune system, THP-1 gene expression was monitored at a transcriptional scale using whole human genome cDNA microarray after stimulation with Mma\_DMAG. The binary logarithm of Mma\_DMAG-stimulated cells *versus* nontreated cells ratios were considered, with adjusted *p* values  $< 0.01$ . The statistical transcriptomic analysis from two independent experiments showed the alteration of 547 genes after 8 h of incubation (supplemental Table S1). The selected genes were classified in functional groups and according to gene ontology using PANTHER (supplemental Table S2).

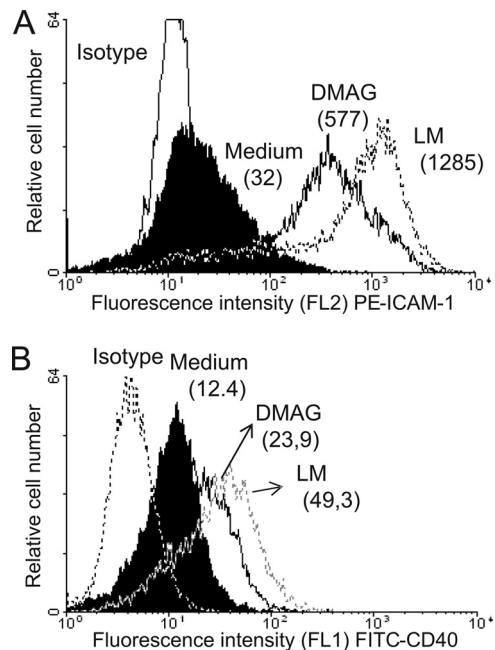


**FIGURE 4. Cell surface antigen expression on THP-1 macrophages stimulated with Mma\_DMAG.** Differentiated THP-1 cells were left untreated (*Medium*) or incubated with 20  $\mu$ g/ml of purified Mma\_DMAG or LM. After 20 h of incubation, ICAM-1 (CD54) (A) and CD40 (B) expression was determined by flow cytometry using PE-conjugated anti-CD54 or FITC-conjugated anti-CD40, respectively. Cells were exposed also with irrelevant antibodies (PE- or FITC-conjugated mouse isotype controls). Results are shown as linear-log scale fluorescence histograms. The mean fluorescence intensity is shown in parentheses. The results presented are from one representative experiment of three independent experiments with similar results.

Compared with a NCBI *Homo sapiens* reference list, the differentially regulated genes (corresponding to significant increased or decreased transcription levels) revealed that some biological processes were significantly over-represented (*p* value  $< 0.05$ ). This was particularly the case for processes related to immune system (167 genes of 547), response to stimuli, cell surface receptor-linked signal transduction pathways and intracellular signaling cascade, cell communication, metabolic systems (particularly nucleic acid and lipid metabolisms), and developmental stages. Interestingly, several overexpressed genes involved in immune responses were relevant to macrophage activation, cell adhesion, endocytosis, apoptosis, angiogenesis, and response to stress and to IFN- $\gamma$ . Cell signaling pathways analysis led to the identification of genes involved in inflammatory mechanisms mediated by chemokines/cytokines and TLR, apoptosis regulation (pro- or anti-), integrin and heterotrimeric G protein signaling pathways, and oxidative stress response as well as growth factors activities. Molecular function and protein class Gene ontology analyses indicated the enrichment of chemokines/cytokines, signaling molecules, transcription factors, enzymes (transferase, hydrolase, kinase, phosphatase, oxygenase), and receptors activities. As reported in Table 2, IL-8, TNF- $\alpha$ , and IL-1 $\beta$  were among the most highly expressed gene candidates (up-regulated 17, 10, and 45 times, respectively, compared with the nontreated macrophages), thus confirming our ELISA results (Fig. 3). In addition, several other genes from the “cytokine/chemokine” family were strongly up-regulated with a sharp preference for the CCL and CXCL chemotactic factors. Several cell surface markers were also strongly up-regulated,

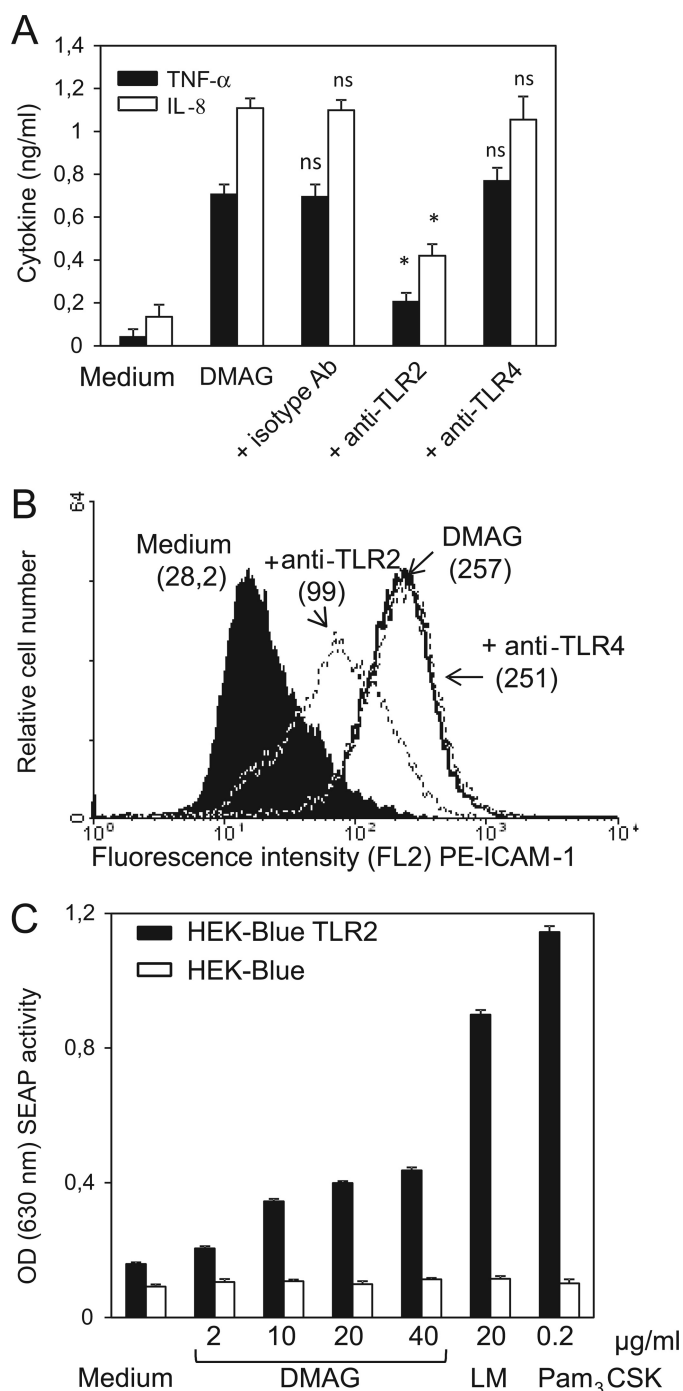


**FIGURE 5. TLR2-dependent activity of Mma\_DMAG.** Differentiated THP-1 cells were pretreated with 15  $\mu$ g/ml concentrations of either anti-TLR2, anti-TLR4, or control isotype monoclonal antibodies (Ab) for 30 min at 37  $^{\circ}$ C in 2% FCS-RPMI 1640 medium before the addition of 20  $\mu$ g/ml Mma\_DMAG. **A**, supernatants were collected after 6 or 24 h and assayed by ELISA for both TNF- $\alpha$  and IL-8 productions. Values represent the means  $\pm$  S.D. of triplicates. Statistical analyses were performed using Student's *t* test. Asterisks indicate values of  $p < 0.02$ ; *ns*, nonspecific  $p > 0.05$ . **B**, cell surface expression of ICAM-1 was determined by flow cytometry after stimulation of differentiated THP-1 cells for 24 h. The shown data are representative of at least of three independent experiments. **C**, stimulation of HEK-Blue-hTLR2 cell line by Mma\_DMAG is shown. The HEK-Blue-hTLR2 and HEK-blue-Null1 (control) cell lines were stimulated with various Mma\_DMAG concentrations. Lipopeptide Pam<sub>3</sub>CSK<sub>4</sub> (200 ng/ml) and LM (20  $\mu$ g/ml) were also included as TLR2 agonists. Cell activation was determined after 20 h of incubation by measuring SEAP activity at OD<sub>630</sub> using the QUANTI-Blue detection assay. Results are expressed as means  $\pm$  S.D. of triplicates and are representative of three independent experiments. Statistical significance between Mma\_DMAG-treated

including ICAM-1 and CD40 (18 and 5 times, respectively), in agreement with their increased cell surface detection by flow cytometry (Fig. 4). Up-regulation of genes related to leukocyte recruitment and activation and to complement activation (pentraxin PTX3, C3AR1) is also of special interest. Moreover, genes coding for enzymes participating in the remodeling of the host matrix, such as matrix metalloproteinases (MMP-1, MMP-9), were found to be up-regulated along with others related to redox process (SOD2, TXNRD1, CYP19A1, HMOX1) and those involved in central metabolic pathways, post-translational modification of glycans (CHST2, CHST7 sulfotransferases and Neu4 sialidase) or in the catabolism of tryptophan (IDO1). Interestingly, a large proportion of these up-regulated genes are known to be overexpressed during mycobacterial infections (57, 58). In addition, several genes down-regulated after exposure of macrophages to Mma\_DMAG (supplemental Table S1) may be relevant to mycobacterial pathogenesis. These include lipidic antigen presentation to CD1d ( $\log_2$  ratio =  $-2.03$ ,  $p < 0.00076$ ), NOD-like receptor family CARD domain containing 3 (called NLRC3,  $\log_2$  ratio =  $-1.38$ ,  $p < 0.006$ ), apoptosis inhibitory protein (NAIP with  $\log_2$  ratio =  $-1.38$ ,  $p < 0.0013$ ), and CXCR2 and CX3CR1 chemokine receptors ( $\log_2$  ratio =  $-1.52$ ,  $p < 0.008$ ,  $\log_2$  ratio =  $-2.02$ ,  $p < 0.0006$ ) as well as ADAM metallopeptidase (ADAMTS5,  $\log_2$  ratio =  $-1.49$ ,  $p < 0.0018$ ) or serpin peptidase inhibitor clade B member2 (SERPINB2,  $\log_2$  ratio =  $-3.19$ ,  $p < 0.0002$ ).

In conclusion, the microarray analysis not only confirms the proinflammatory-inducing activity of Mma\_DMAG but also suggests that Mma\_DMAG affects expression of a large panoply of macrophage genes that are connected to the immunopathogenesis of mycobacterial infections, with important pathways related to signaling events, inflammation, lipid antigen presentation, or tissue destruction.

## DISCUSSION

Based on structural analogy with mAGP and studies on the action of anti-tubercular drugs, a metabolic relationship between DMAG from *M. bovis* BCG and mAGP has recently been highlighted (33). However, neither the metabolic pathway leading to DMAG nor its potential biological properties has been reported yet. We present here the detailed structural elucidation of the 5-*O*-mycolyl- $\beta$ -Araf-(1 $\rightarrow$ 2)-5-*O*-mycolyl- $\alpha$ -Araf-(1 $\rightarrow$ 1)-Gro (DMAG) in *Mma* and provide the first biological functions of this cell wall-associated glycolipid. A combination of NMR spectroscopy and mass spectrometry revealed the presence of three mycolate subclasses ( $\alpha$ -, keto-, and methoxy-mycolic acids) in Mma\_DMAG (33). Furthermore, in contrast to *M. tuberculosis* that contains a ratio of  $\alpha$ -mycolates/oxygenated mycolates (*i.e.* methoxy- and keto-mycolates) of 1/1 (59), oxygenated mycolates are predominant in Mma\_DMAG. It is noteworthy that exogenous glycerol is required to stimulate DMAG production (33) as reported earlier for another glycolipid, GroMM (60). These observations

and unstimulated HEK-Blue-hTLR2 cells was determined using Student's *t* test ( $p$  values were  $< 0.03$ ).



## Proinflammatory Activity of Mycobacterial DMAG

**TABLE 2**

Microarray analyses; genes up-regulated in human macrophages-like THP1 cells after stimulation for 8 h with Mma\_DMAG

The complete list of altered gene expression was available in supplemental Table S1.

Gene	Description	Log <sub>2</sub> ratio <sup>a</sup>
<b>Cell surface antigen</b>		
ICAM1	Intercellular adhesion molecule 1	4.20
VCAM1	Vascular cell adhesion molecule 1	2.84
CD40	CD40 molecule, TNF receptor superfamily member 5	2.49
CD83	CD83 molecule	3.06
CD44	CD44 molecule (Indian blood group)	2.07
ITGB8	Integrin, $\beta$ 8	2.04
SLAMF7	Signaling lymphocytic activation molecule family member 7	3.86
<b>Protease/metalloproteinase</b>		
MMP1	Matrix metalloproteinase 1 (interstitial collagenase)	4.95
MMP9	Matrix metalloproteinase 9 (gelatinase B, 92-kDa gelatinase, 92-kDa type IV collagenase)	3.25
PCSK5	Proprotein convertase subtilisin/kexin type 5	2.91
<b>Chemokines-cytokines</b>		
CCL8 (MCP-2)	Chemokine ligand 8	5.94
CCL2 (MCP-1)	Chemokine ligand 2	4.91
CXCL2 (MIP-2)	Chemokine ligand 2	4.62
CXCL1	Chemokine ligand 1	4.31
CCL4 (MIP-1)	Chemokine ligand 4	4.07
CCL20	Chemokine ligand 20	4.00
CXCL11	Chemokine ligand 11	3.70
CXCL3(GRO)	Chemokine ligand 3	3.65
CXCL10	Chemokine ligand 10	3.58
CCL7	Chemokine ligand 7	3.41
CCL3L3	Chemokine ligand 3-like 3	3.37
CXCL9	Chemokine ligand 9	2.02
IL-8	Interleukin 8	4.11
IL-1 $\beta$	Interleukin 1, $\beta$	5.54
TNF $\alpha$	Tumor necrosis factor	3.33
IL-1 $\alpha$	Interleukin 1, $\alpha$	2.42
<b>Cytokine receptors</b>		
CCR7	Chemokine (C-C motif) receptor 7	4.18
IL18RAP	Interleukin 18 receptor accessory protein	3.17
CMKLR1	Chemokine-like receptor 1	2.37
<b>Apoptosis</b>		
BCL2A1	BCL2-related protein A1	3.34
TNFAIP3	Tumor necrosis factor, $\alpha$ -induced protein 3	3.25
IER3	Immediate early response 3	3.33
<b>Redox-enzymes</b>		
CYP19A1	Cytochrome P450, family 19, subfamily A, polypeptide 1	3.27
SOD2	Superoxide dismutase 2, mitochondrial	3.18
<b>Cell signaling pathways/nuclear factors</b>		
RGS1	Regulator of G-protein signaling 1	4.01
NR4A3	Nuclear receptor subfamily 4, group A, member 3	3.92
RND3	Rho family GTPase 3	3.70
TNIP3	TNFAIP3 interacting protein 3	3.23
TNFAIP3	Tumor necrosis factor, $\alpha$ -induced protein 3	3.25
RCAN1	Regulator of calcineurin 1	3.16
SOCS3	Suppressor of cytokine signaling 3	3.09
DUSP1	Dual specificity phosphatase 1	3.04
RGS16	Regulator of G-protein signaling 16	2.96
STAT4	Signal transducer and activator of transcription 4	2.73
ATF3	Activating transcription factor 3	2.75
TRAF1	TNF receptor-associated factor 1	2.68
BCL3	B-cell CLL/lymphoma 3	2.28
SPHK1	Sphingosine kinase 1	2.16
NFKB2	Nuclear factor of $\kappa$ light polypeptide gene enhancer	2.10
NFKB1	Nuclear factor of $\kappa$ light polypeptide gene enhancer	2.19
NFKBIZ	Nuclear factor of $\kappa$ light polypeptide gene enhancer	2.46
<b>IFN-inducible protein</b>		
IFIT3	Interferon-induced protein	3.24
IFIT2	Interferon-induced protein	2.50
IFIT1	Interferon-induced protein	2.4
IFIT5	Interferon-induced protein	2.17
<b>Transporters/channels</b>		
AQP9	Aquaporin 9	3.66
SLC7A11	Solute carrier family 7	2.51
SLC7A11	ATPase, Ca <sup>2+</sup> transporting, plasma membrane 1	2.27
<b>Lipid<sup>b</sup> and amino acid<sup>c</sup> metabolism</b>		
FABP4 <sup>b</sup>	Fatty acid-binding protein 4	3.38
AGPAT9 <sup>b</sup>	1-Acylglycerol-3-phosphate O-acyltransferase 9	3.13
PTGS2 <sup>b</sup>	Prostaglandin-endoperoxide synthase 2	3.17
MGLL <sup>b</sup>	Monoglyceride lipase	3.07
PLA2G7 <sup>b</sup>	Phospholipase A2, group VII	2.78

TABLE 2—continued

Gene	Description	Log <sub>2</sub> ratio <sup>a</sup>
ACSL1 <sup>b</sup>	Acyl-CoA synthetase long-chain family member 1	2.36
LRP12 <sup>b</sup>	Low density lipoprotein receptor-related protein 12	2.11
IDO1 <sup>c</sup>	Indoleamine 2,3-dioxygenase 1 (Trp catabolism)	2.78
KYNU <sup>c</sup>	Kynureninase (L-kynurenine hydrolase)	2.36
<b>Carbohydrate metabolism</b>		
CHST7	Carbohydrate (N-acetylglucosamine 6-O) sulfotransferase 7	2.42
CHST2	Carbohydrate (N-acetylglucosamine-6-O) sulfotransferase 2	2.12
NEU4	Sialidase 4	2.26
SDC4	Syndecan 4	2.22
<b>Nucleic metabolism</b>		
PDE4B	Phosphodiesterase 4B, cAMP-specific	2.59
NTSE	5'-Nucleotidase, ecto (CD73)	2.35
NAMPT	Nicotinamide phosphoribosyltransferase	2.27
ADORA2A	Adenosine A2a receptor	2.85
ADAD2	Adenosine deaminase domain containing 2	2.83
<b>Miscellaneous</b>		
EBI3	Epstein-Barr virus-induced 3	3.65
EGR2	Early growth response 2	3.29
SERPINE2	Serpin peptidase inhibitor, serpin peptidase inhibitor, clade E (nexin, plasminogen activator inhibitor type 1), member 2	3.24
HBEGF	Heparin binding EGF-like growth factor	2.03

<sup>a</sup> Binary log ratio of altered gene expression according to microarray analysis of macrophages after exposure for 8 h with DMAG compared to unstimulated cells. Results with a log<sub>2</sub> ratio >2 are shown and are representative of two independent experiments.

<sup>b</sup> Genes related to lipid metabolism.

<sup>c</sup> Genes related to amino acid metabolism.

have led to the speculation that DMAG may result from the catabolism of already-synthesized mAGP following the action of an arabinanase and subsequent transfer onto an endo- or exogenous substrate, such as glycerol (33). During infection of foamy macrophages, dynamic changes in the glycolipid composition of the mycobacterial cell wall have been reported to occur (61, 62). That these mechanisms may be responsible *in vivo* for the production of DMAG during infection remains, however, to be demonstrated.

Considering the high structural analogy between DMAG and TDM as well as its localization to the mycobacterial cell wall (presumably surface-exposed), we reasoned that DMAG may share with TDM several traits that are relevant to mycobacterial pathogenesis, such as proinflammatory cytokine production and formation of granuloma and tissue-destructive lesions (63). Mma\_DMAG was found to stimulate a potent macrophage inflammatory response. This contrasts to LOS from Mma (40) that were found to inhibit the secretion of TNF- $\alpha$  from LPS-stimulated macrophages (45). The Mma\_DMAG-mediated inflammatory response was dependent at least partly on ligation to TLR2. This interaction results in the induction of TNF- $\alpha$ , IL-1 $\beta$ , and IL-8 secretion and triggers macrophage activation by inducing expression of cell surface antigens such as ICAM-1 or CD40. These results were subsequently extended at a whole transcriptomic level. Microarray studies performed on macrophages exposed to DMAG indicate that many genes participating in inflammation or chemotaxis are up-regulated, which are relevant to granuloma formation. Altogether, these factors are crucial in tipping the balance between intracellular survival of bacteria and their eventual elimination by antimicrobial mechanisms of activated macrophages (64, 65). Our findings emphasize a potential function of DMAG in modulation of the host immune response, as previously suggested by Honda *et al.* (34). Indeed, the presence of a humoral anti-DMAG response has been detected in patients infected by *M. avium* or *M. tuberculosis*, suggesting that DMAG may be

regarded as an immunogenic glycolipid (34). Given the high structural relatedness with other mycolic acid-bearing molecules, it is not surprising that DMAG triggers activity on immune cells. Indeed, arabino-mycolates obtained by acid hydrolysis from the cell-wall skeleton of *M. bovis* BCG (BCG-CWS) (66) as well as synthesized arabino-mycolates (67) have been shown to induce TNF- $\alpha$  production in murine macrophage cell lines. Moreover, these compounds, described as potent adjuvant *in vivo*, enhanced delayed type hypersensitivity reactions against inactivated tumor cells (66). A 5-mycoloyl diarabinoside isolated from the cell wall of *M. tuberculosis* was also reported to act as potential endotoxins through an inhibitory activity on mitochondrial oxidative phosphorylation (68). Arabinosylated mycolic acid isolated from *M. bovis* BCG were proposed to participate to acute inflammatory response, essentially as a consequence of a constant and massive recruitment of polymorphonuclear leukocytes (69). Furthermore, *cis*- or *trans*-cyclopropanated mycolic acids in TDM were found to directly regulate the innate immune activation of macrophages by modulating TNF- $\alpha$  production (29, 71). Interestingly, the molecular structure of mycolic acid seems to influence the pattern of inflammatory response (72). Thus, TDM lacking *trans*-cyclopropane rings purified from a *M. tuberculosis* cyclopropane-mycolic acid synthase 2 (*cmaA2*) null mutant was 5 times more potent in stimulating macrophages than TDM obtained from the wild-type strain (29, 71). In contrast, *trans*-cyclopropanation of mycolic acids on TDM suppresses *M. tuberculosis*-induced inflammation and virulence (29, 71). These authors have also suggested that *cis*-cyclopropanation of TDM was critical to its proinflammatory activity. Furthermore, a mutant of *MmaA4* gene (methoxy mycolic acid synthase 4) was associated with higher production of TNF- $\alpha$  and IL-12 compared with the wild-type *M. tuberculosis* strain (73). A recent study also emphasized the fact that free methoxy- and keto-mycolic acid with *cis*-cyclopropane stereochemistry elicited high and mild inflammatory responses, respectively, whereas  $\alpha$ -mycolates

## Proinflammatory Activity of Mycobacterial DMAG

were inactive (72). Therefore, the structure of three subclasses of *cis*-cyclopropanated mycolates (keto, methoxy, and  $\alpha$ ) found in Mma\_DMAG and the lack of *trans*-cyclopropanation are in favor of our biological results, demonstrating that DMAG may display an inflammatory pattern on the immune innate response. From a mechanistic point of view, our results indicate that DMAG-induced activation of macrophages is dependent on TLR2, presumably through an interaction with mycolic acids, as reported for arabino-mycolates of *M. bovis* BCG (BCG-CWS) (66). However, because both TNF- $\alpha$  and IL-8 responses were partially inhibited in the presence of neutralizing TLR-2 antibodies, one can presume that host recognition of DMAG involves additional receptors. This was reported for TDM, which binds to multiple receptors, including TLR2/MARCO/CD14 complex or the Mincle C-type lectin (25–28). However, that DMAG binds to Mincle is very unlikely, as the trehalose unit of TDM has been demonstrated to be crucial to the binding of TDM to Mincle (25, 27–29).

Besides TDM and arabinose monomycolate, other glycolipids display structural similarity to DMAG, such GroMM. GroMM purified from *M. tuberculosis* was presented as an antigenic glycolipid, potent stimulator of CD1b-restricted CD4<sup>+</sup> T cell clones (47). Presentation of free mycolates, GMM, or GroMM by CD1 molecules triggers the T cell responses, leading to the development of acquired immunity against mycobacteria (61, 74, 75). GroMM induces eosinophilic hypersensitivity responses in guinea pigs, which led the authors to predict that the host response to this lipid produced by dormant mycobacteria contributes to their survival in the host through the expression of T helper (Th)2-type cytokines, such as IL-5 and IL-10 (60). GroMM biosynthesis pathway has not been elucidated yet; thus, the metabolic relationship between DMAG and GroMM cannot be inferred. Interestingly, we established that activation of differentiated THP-1 cells by Mma\_DMAG was accompanied by the down-regulation of CD1d transcript, an antigen restricted to natural killer T cells activation. Although this result has to be confirmed experimentally, it suggests that DMAG could also modulate the effectiveness of lipidic antigen presentation to natural killer T cells. In agreement with our results, Roura-Mir *et al.* (76) previously demonstrated that the mycobacterial cell wall lipids of *M. tuberculosis* that activate human monocytes through TLR2 up-regulated CD1a, CD1b, and CD1c gene and protein expression, whereas CD1d transcripts decreased on the first day after exposure to the lipids.

Overall, this study illustrates the broad inflammatory activity of Mma\_DMAG. As such, it describes a new partner in the growing list of mycobacterial cell wall components able to modulate the host immune response. Whether this activity ultimately leads to the recruitment of immune cells, eventually conditioning the outcome of the infection, remains to be established. Future work will be dedicated to address the *in vivo* biological relevance of DMAG activity and its potential participation in formation and/or maintenance of the granuloma. This is now possible thanks to the use of zebrafish embryos, which enable the investigation the *Mma* infection process at a spatiotemporal level (3, 77). As an example of application, phagocyte recruitments and granu-

loma formation could be readily visualized in real time by intravenously injecting Mma\_DMAG-conjugated fluorescent beads in zebrafish embryos.

Recent reports have highlighted the possibility of producing novel classes of chemically defined lipid adjuvants (66, 70). For instance, the immunostimulatory activities of arabino-mycolates (65) and GroMM from *M. bovis* BCG (70) have been proposed to enhance the activity of new vaccine formulations. Based on the structural similarity between these compounds and DMAG, one can presume that DMAG elicits a potent adjuvant activity to be exploited, although this perspective of application requires a more extensive characterization of DMAG immunostimulatory properties.

---

*Acknowledgments*—We are grateful to Marlène Mortuaire for technical advice in cell culture. We are also grateful to W. Bitter and A. van der Sar for kindly providing Mma7.

---

## REFERENCES

1. Daffé, M., and Draper, P. (1998) The envelope layers of mycobacteria with reference to their pathogenicity. *Adv. Microb. Physiol.* **39**, 131–203
2. Stinear, T. P., Seemann, T., Harrison, P. F., Jenkin, G. A., Davies, J. K., Johnson, P. D., Abdellah, Z., Arrowsmith, C., Chillingworth, T., Churcher, C., Clarke, K., Cronin, A., Davis, P., Goodhead, I., Holroyd, N., Jagels, K., Lord, A., Moule, S., Mungall, K., Norbertczak, H., Quail, M. A., Rabinowitsch, E., Walker, D., White, B., Whitehead, S., Small, P. L., Brosch, R., Ramakrishnan, L., Fischbach, M. A., Parkhill, J., and Cole, S. T. (2008) Insights from the complete genome sequence of *Mycobacterium marinum* on the evolution of *Mycobacterium tuberculosis*. *Genome Res.* **18**, 729–741
3. Ramakrishnan, L. (1994) Using *Mycobacterium marinum* and its hosts to study tuberculosis. *Infect. Immun.* **62**, 3222–3229
4. Petrini, B. (2006) *Mycobacterium marinum*. Ubiquitous agent of waterborne granulomatous skin infections. *Eur. J. Clin. Microbiol. Infect. Dis.* **25**, 609–613
5. Swaim, L. E., Connolly, L. E., Volkman, H. E., Humbert, O., Born, D. E., and Ramakrishnan, L. (2006) *Mycobacterium marinum* infection of adult zebrafish causes caseating granulomatous tuberculosis and is moderated by adaptive immunity. *Infect. Immun.* **74**, 6108–6117
6. Gao, L. Y., Groger, R., Cox, J. S., Beverley, S. M., Lawson, E. H., and Brown, E. J. (2003) Transposon mutagenesis of *Mycobacterium marinum* identifies a locus linking pigmentation and intracellular survival. *Infect. Immun.* **71**, 922–929
7. Tobin, D. M., and Ramakrishnan, L. (2008) Comparative pathogenesis of *Mycobacterium marinum* and *Mycobacterium tuberculosis*. *Cell Microbiol.* **10**, 1027–1039
8. Davis, J. M., Clay, H., Lewis, J. L., Ghori, N., Herbomel, P., and Ramakrishnan, L. (2002) Real-time visualization of mycobacterium-macrophage interactions leading to initiation of granuloma formation in zebrafish embryos. *Immunity* **17**, 693–702
9. Cosma, C. L., Humbert, O., and Ramakrishnan, L. (2004) Superinfecting mycobacteria home to established tuberculous granulomas. *Nat. Immunol.* **5**, 828–835
10. Cosma, C. L., Swaim, L. E., Volkman, H., Ramakrishnan, L., and Davis, J. M. (2006) Zebrafish and frog models of *Mycobacterium marinum* infection. *Curr. Protoc. Microbiol.*, Chapter 10, Unit 10B.2
11. Volkman, H. E., Clay, H., Beery, D., Chang, J. C., Sherman, D. R., and Ramakrishnan, L. (2004) Tuberculous granuloma formation is enhanced by a mycobacterium virulence determinant. *PLoS Biol.* **2**, e367
12. Clay, H., Davis, J. M., Beery, D., Huttenlocher, A., Lyons, S. E., and Ramakrishnan, L. (2007) Dichotomous role of the macrophage in early *Mycobacterium marinum* infection of the zebrafish. *Cell Host Microbe* **2**, 29–39
13. Tobin, D. M., Vary, J. C., Jr., Ray, J. P., Walsh, G. S., Dunstan, S. J., Bang,



- N. D., Hagge, D. A., Khadge, S., King, M. C., Hawn, T. R., Moens, C. B., and Ramakrishnan, L. (2010) The *Ith4h* locus modulates susceptibility to mycobacterial infection in zebrafish and humans. *Cell* **140**, 717–730
14. Davis, J. M., and Ramakrishnan, L. (2009) The role of the granuloma in expansion and dissemination of early tuberculosis infection. *Cell* **136**, 37–49
  15. Kremer, L., Baulard, A., and Besra, G. S. (2000) in *Molecular Genetics of Mycobacteria* (Hatfull, G. F., and Jacobs, W. R., Jr., ed.) pp. 173–190, American Society for Microbiology, Washington, D. C.
  16. Ryll, R., Kumazawa, Y., and Yano, I. (2001) Mycobacterial cord factor, but not sulfolipid, causes depletion of NKT cells and up regulation of CD1d1 on murine macrophages. *Microbiol. Immunol.* **45**, 801–811
  17. Chatterjee, D., and Khoo, K. H. (2001) The surface of glycopeptidolipids of mycobacteria. Structures and biological properties. *Cell. Mol. Life Sci.* **58**, 2018–2042
  18. Briken, V., Porcelli, S. A., Besra, G. S., and Kremer, L. (2004) Mycobacterial lipoarabinomannan and related lipoglycans from biogenesis to modulation of the immune response. *Mol. Microbiol.* **53**, 391–403
  19. Karakousis, P. C., Bishai, W. R., and Dorman, S. E. (2004) *Mycobacterium tuberculosis* cell envelope lipids and the host immune response. *Cell. Microbiol.* **6**, 105–116
  20. Astarie-Dequeker, C., Nigou, J., Passemar, C., and Guilhot, C. (2010) in *Drug Discovery Today: Disease Mechanisms*, 7th Ed., pp. e33–e41, Elsevier Science Publishing Co., Inc., New York
  21. Hunter, R. L., Olsen, M. R., Jagannath, C., and Actor, J. K. (2006) Multiple roles of cord factor in the pathogenesis of primary, secondary, and cavitary tuberculosis, including a revised description of the pathology of secondary disease. *Ann. Clin. Lab. Sci.* **36**, 371–386
  22. Rajni, Rao, N., and Meena, L. S. (2011) Biosynthesis and virulent behavior of lipids produced by *Mycobacterium tuberculosis*. LAM and cord factor. An Overview. *Biotechnol. Res. Int.* 274693
  23. Geisel, R. E., Sakamoto, K., Russell, D. G., and Rhoades, E. R. (2005) *In vivo* activity of released cell wall lipids of *Mycobacterium bovis* bacillus Calmette-Guerin is due principally to trehalose mycolates. *J. Immunol.* **174**, 5007–5015
  24. Welsh, K. J., Abbott, A. N., Hwang, S. A., Indrigo, J., Armitage, L. Y., Blackburn, M. R., Hunter, R. L., Jr., and Actor, J. K. (2008) A role of TNF- $\alpha$ , complement C5, and IL-6 in the initiation and development of the mycobacterial cord factor trehalose 6,6'-dimycolate induced granulomatous response. *Microbiology* **154**, 1813–1824
  25. Yamasaki, S., Ishikawa, E., Sakuma, M., Hara, H., Ogata, K., and Saito, T. (2008) Mincle is an ITAM-coupled activating receptor that senses damaged cells. *Nat. Immunol.* **9**, 1179–1188
  26. Bowdish, D. M., Sakamoto, K., Kim, M. J., Kroos, M., Mukhopadhyay, S., Leifer, C. A., Tryggvason, K., Gordon, S., and Russell, D. G. (2009) MARCO, TLR2, and CD14 are required for macrophage cytokine responses to mycobacterial trehalose dimycolate and *Mycobacterium tuberculosis*. *PLoS Pathog.* **5**, e1000474
  27. Ishikawa, E., Ishikawa, T., Morita, Y. S., Toyonaga, K., Yamada, H., Takeuchi, O., Kinoshita, T., Akira, S., Yoshikai, Y., and Yamasaki, S. (2009) Direct recognition of the mycobacterial glycolipid, trehalose dimycolate by C-type lectin Mincle. *J. Exp. Med.* **206**, 2879–2888
  28. Matsunaga, I., and Moody, D. B. (2009) Mincle is a long sought receptor for mycobacterial cord factor. *J. Exp. Med.* **206**, 2865–2868
  29. Rao, V., Gao, F., Chen, B., Jacobs, W. R., Jr., and Glickman, M. S. (2006) Trans cyclopanation of mycolic acids on trehalose dimycolate suppresses *Mycobacterium tuberculosis*-induced inflammation and virulence. *J. Clin. Invest.* **116**, 1660–1667
  30. Fujita, Y., Okamoto, Y., Uenishi, Y., Sunagawa, M., Uchiyama, T., and Yano, I. (2007) Molecular and supramolecular structure related differences in toxicity and granulomatogenic activity of mycobacterial cords factor in mice. *Microb. Pathog.* **43**, 10–21
  31. Watanabe, M., Kudoh, S., Yamada, Y., Iguchi, K., and Minnikin, D. E. (1992) A new glycolipid from *Mycobacterium avium-Mycobacterium intracellulare* complex. *Biochim. Biophys. Acta* **1165**, 53–60
  32. Watanabe, M., Aoyagi, Y., Ohta, A., and Minnikin, D. E. (1997) Structures of phenolic glycolipids from *Mycobacterium kansasii*. *Eur. J. Biochem.* **248**, 93–98
  33. Rombouts, Y., Brust, B., Ojha, A. K., Maes, E., Coddeville, B., Ellass-Rochard, E., Kremer, L., and Guerardel, Y. (2012) Exposure of mycobacteria to cell wall inhibitory drugs decreases production of arabinoglycerolipid related to mycolyl-arabinogalactan-peptidoglycan. *J. Biol. Chem.* **287**, 11060–11069
  34. Honda, I., Kawajiri, K., Watanabe, M., Toida, I., Kawamata, K., and Minnikin, D. E. (1993) Evaluation of the use of 5-mycoloyl- $\beta$ -arabinofuranosyl-(1-2)-5-mycoloyl- $\alpha$ -arabinofuranosyl-(1-1')-glycerol in serodiagnosis of *Mycobacterium aviumintracellulare* complex infection. *Res. Microbiol.* **144**, 229–235
  35. Puttinaowarat, S., Thompson, K., Lilley, J., and Adams, A. (1999) Characterization of *Mycobacterium* spp isolated from fish by pyrolysis mass spectrometry (PyMS) analysis. *AAHRI (Aquatic Animal Health Research Institute) Newslett.* **8**, 4–8
  36. Burguière, A., Hitchen, P. G., Dover, L. G., Kremer, L., Ridell, M., Alexander, D. C., Liu, J., Morris, H. R., Minnikin, D. E., Dell, A., and Besra, G. S. (2005) *LosA*, a key glycosyltransferase involved in the biosynthesis of a novel family of glycosylated acyltrehalose lipooligosaccharides from *Mycobacterium marinum*. *J. Biol. Chem.* **280**, 42124–42133
  37. Guerardel, Y., Maes, E., Ellass, E., Leroy, Y., Timmerman, P., Besra, G. S., Locht, C., Strecker, G., and Kremer, L. (2002) Structural study of lipomannan and lipoarabinomannan from *Mycobacterium chelonae*. Presence of unusual components with alpha 1,3-mannopyranose side chains. *J. Biol. Chem.* **277**, 30635–30648
  38. Kremer, L., Guérardel, Y., Gurcha, S. S., Locht, C., and Besra, G. S. (2002) Temperature-induced changes in the cell-wall components of *Mycobacterium thermoresistibile*. *Microbiology* **148**, 3145–3154
  39. Dover, L. G., Alahari, A., Grattraud, P., Gomes, J. M., Bhowruth, V., Reynolds, R. C., Besra, G. S., and Kremer, L. (2007) *EthA*, a common activator of thiocarbamide-containing drugs acting on different mycobacterial targets. *Antimicrob. Agents Chemother.* **51**, 1055–1063
  40. Rombouts, Y., Ellass, E., Biot, C., Maes, E., Coddeville, B., Burguière, A., Tokarski, C., Buisine, E., Trivelli, X., Kremer, L., and Guérardel, Y. (2010) Structural analysis of an unusual bioactive *N*-acylated lipo-oligosaccharide LOS-IV in *Mycobacterium marinum*. *J. Am. Chem. Soc.* **132**, 16073–16084
  41. Ihaka, R., and Gentleman, R. R. (1996) A language for data analysis and graphics. *J. Comput. Graph. Stat.* **5**, 299–314
  42. Smyth, G. K., Yang, Y. H., and Speed, T. (2003) Statistical issues in cDNA microarray data analysis. *Methods Mol. Biol.* **224**, 111–136
  43. Yang, Y. H., Dudoit, S., Luu, P., Lin, D. M., Peng, V., Ngai, J., and Speed, T. P. (2002) Normalization for cDNA microarray data. A robust composite method addressing single and multiple slide systematic variation. *Nucleic Acids Res.* **30**, e15
  44. Lönnstedt, I., and Speed, T. P. (2002) Replicated microarray data. *Statistica Sinica* **12**, 31–46
  45. Rombouts, Y., Burguière, A., Maes, E., Coddeville, B., Ellass, E., Guérardel, Y., and Kremer, L. (2009) *Mycobacterium marinum* lipooligosaccharides are unique caryophyllose-containing cell wall glycolipids that inhibit tumor necrosis factor  $\alpha$  secretion in macrophages. *J. Biol. Chem.* **284**, 20975–20988
  46. Daffé, M., Lanéelle, M. A., and Lacave, C. (1991) Structure and stereochemistry of mycolic acids of *Mycobacterium marinum* and *Mycobacterium ulcerans*. *Res. Microbiol.* **142**, 397–403
  47. Layre, E., Collmann, A., Bastian, M., Mariotti, S., Czapllicki, J., Prandi, J., Mori, L., Stenger, S., De Libero, G., Puzo, G., and Gilleron, M. (2009) Mycolic acids constitute a scaffold for mycobacterial lipid antigens stimulating CD1-restricted T cells. *Chem. Biol.* **16**, 82–92
  48. Chensue, S. W., Warmington, K. S., Ruth, J. H., Lincoln, P., and Kunkel, S. L. (1995) Cytokine function during mycobacterial and schistosomal antigen-induced pulmonary granuloma formation. Local and regional participation of IFN- $\gamma$ , IL-10, and TNF. *J. Immunol.* **154**, 5969–5976
  49. Algood, H. M., Lin, P. L., and Flynn, J. L. (2005) TNF  $\alpha$  and chemokine interactions in the formation and maintenance of granulomas in tuberculosis. *Clin. Infect. Dis.* **41**, S189–S193
  50. Chensue, S. W., Davey, M. P., Remick, D. G., and Kunkel, S. (1986) Release of interleukin-1 by peripheral blood mononuclear cells in patients with tuberculosis and active inflammation. *Infect. Immun.* **52**, 341–343

51. Kleinnijenhuis, J., Joosten, L. A., van de Veerdonk, F. L., Savage, N., van Crevel, R., Kullberg, B. J., van der Ven, A., Ottenhoff, T. H., Dinarello, C. A., van der Meer, J. W., and Netea, M. G. (2009) Transcriptional and inflammasome-mediated pathways for the induction of IL-1 $\beta$  production by *Mycobacterium tuberculosis*. *Eur. J. Immunol.* **39**, 1914–1922
52. Vignal, C., Guérardel Y., Kremer L., Masson M., Legrand D., Mazurier J., and Ellass, E. (2003) Lipomannans, but not lipoarabinomannans, purified from *Mycobacterium chelonae* and *Mycobacterium kansasii* induce TNF and IL-8 secretion by a CD14-Toll like receptor 2-dependent mechanisms. *J. Immunol.* **171**, 2014–2023
53. Estrella, J. L., Kan-Sutton, C., Gong, X., Rajagopalan, M., Lewis, D. E., Hunter, R. L., Eissa, N. T., and Jagannath, C. (2011) A novel *in vitro* human macrophage model to study the persistence of *Mycobacterium tuberculosis* using vitamin D(3) and retinoic acid-activated THP-1 macrophages. *Front. Microbiol.* **2**, 67–71
54. Gilleron M., Nigou J., Nicolle, D., Quesniaux, V., and Puzo, G. (2006) The acylation state of mycobacterial lipomannans modulates innate immunity response through toll-like receptor 2. *Chem. Biol.* **13**, 39–47
55. Quesniaux, V. J., Nicolle, D. M., Torres, D., Kremer, L., Guérardel, Y., Nigou, J., Puzo, G., Erard, F., and Ryffel, B. (2004) Toll-like receptor 2 (TLR2)-dependent-positive and TLR2-independent-negative regulation of proinflammatory cytokines by mycobacterial lipomannans. *J. Immunol.* **172**, 4425–4434
56. Lebedeva, T., Dustin, M. L., and Sykulev, Y. (2005) ICAM-1 co-stimulates target cells to facilitate antigen presentation. *Curr. Opin. Immunol.* **17**, 251–258
57. Nau, G. J., Richmond, J. F., Schlesinger, A., Jennings, E. G., Lander, E. S., and Young, R. A. (2002) Human macrophage activation programs induced by bacterial pathogens. *Proc. Natl. Acad. Sci. U.S.A.* **99**, 1503–1508
58. Thuong, N. T., Dunstan, S. J., Chau, T. T., Thorsson, V., Simmons, C. P., Quyen, N. T., Thwaites, G. E., Thi Ngoc Lan, N., Hibberd, M., Teo, Y. Y., Seielstad, M., Aderem, A., Farrar, J. J., and Hawn, T. R. (2008) Identification of tuberculosis susceptibility genes with human macrophage gene expression profiles. *PLoS Pathog.* **4**, e1000229
59. Watanabe, M., Aoyagi, Y., Ridell, M., and Minnikin, D. E. (2001) Separation and characterization of individual mycolic acids in representative mycobacteria. *Microbiology* **147**, 1825–1837
60. Hattori, Y., Matsunaga, I., Komori, T., Urakawa, T., Nakamura, T., Fujiwara, N., Hiromatsu, K., Harashima, H., and Sugita, M. (2011) Glycerol monomycolate, a latent tuberculosis-associated mycobacterial lipid, induces eosinophilic hypersensitivity responses in guinea pigs. *Biochem. Biophys. Res. Commun.* **409**, 304–307
61. Ehrt, S., and Schnappinger, D. (2007) *Mycobacterium tuberculosis* virulence. Lipids inside and out. *Nat. Med.* **13**, 284–285
62. Pandey, A. K., and Sasseti, C. M. (2008) Mycobacterial persistence requires the utilization of host cholesterol. *Proc. Natl. Acad. Sci. U.S.A.* **105**, 4376–4380
63. Khan, A. A., Stocker, B. L., and Timmer, M. S. (2012) Trehalose glycolipids synthesis and biological activities. *Carbohydr. Res.* **356**, 25–36
64. Flynn, J. L., and Chan, J. (2001) Immunology of tuberculosis. *Annu. Rev. Immunol.* **19**, 93–129
65. Raja, A. (2004) Immunology of tuberculosis. *Indian J. Med. Res.* **120**, 213–232
66. Miyauchi, M., Murata, M., Shibuya, K., Koga-Yamakawa, E., Uenishi, Y., Kusunose, N., Sunagawa, M., Yano, I., and Kashiwazaki, Y. (2011) Arabinomycolates derived from the cell-wall skeleton *Mycobacterium bovis* BCG as a prominent structure for recognition by host immunity. *Drug Discov. Ther.* **5**, 130–135
67. Ishiwata, A., Akao, H., Ito, Y., Sunagawa, M., Kusunose, N., and Kashiwazaki, Y. (2006) Synthesis and TNF- $\alpha$  inducing activities of mycolyl-arabinan motif of mycobacterial cell wall components. *Bioorg. Med. Chem.* **14**, 3049–3061
68. Rouanet, J. M., and Laneelle, G. (1983) Mycobacteria arabinolipids as potential endotoxins. Their activity on mitochondrial oxidative phosphorylation. *Ann. Microbiol. (Paris)* **134B**, 233–239
69. Silva, C. L. (1985) Inflammation induced by mycolic acid-containing glycolipids of *Mycobacterium bovis* (BCG). *Braz. J. Med. Biol. Res.* **18**, 327–335
70. Andersen, C. A., Rosenkrands, I., Olsen, A. W., Nordly, P., Christensen, D., Lang, R., Kirschning, C., Gomes, J. M., Bhowruth, V., Minnikin, D. E., Besra, G. S., Follmann, F., Andersen, P., and Agger, E. M. (2009) Novel generation mycobacterial adjuvant based on liposome-encapsulated monomycolyl glycerol from *Mycobacterium bovis* bacillus Calmette-Guérin. *J. Immunol.* **183**, 2294–2302
71. Rao, V., Fujiwara, N., Porcelli, S. A., and Glickman, M. S. (2005) *Mycobacterium tuberculosis* controls host innate immune activation through cyclopropane modification of a glycolipid effector molecule. *J. Exp. Med.* **201**, 535–543
72. Vander Beken, S., Al Dulayymi, J. R., Naessens, T., Koza, G., Maza-Iglesias, M., Rowles, R., Theunissen, C., De Medts, J., Lanckacker, E., Baird, M. S., and Grooten J. (2011) Molecular structure of the *Mycobacterium tuberculosis* virulence factor, mycolic acid, determines the elicited inflammatory pattern. *Eur. J. Immunol.* **41**, 450–460
73. Dao, D. N., Sweeney, K., Hsu, T., Gurucha, S. S., Nascimento, I. P., Roshevsky, D., Besra, G. S., Chan, J., Porcelli, S. A., and Jacobs, W. R. (2008) Mycolic acid modification by the *mmaA4* gene of *M. tuberculosis* modulates IL-12 production. *PLoS Pathog.* **4**, e1000081
74. Matsunaga, I., Naka, T., Talekar, R. S., McConnell, M. J., Katoh, K., Nakao, H., Otsuka, A., Behar, S. M., Yano, I., Moody, D. B., and Sugita, M. (2008) Mycolyltransferase-mediated glycolipid exchange in mycobacteria. *J. Biol. Chem.* **283**, 28835–28841
75. Komori, T., Nakamura, T., Matsunaga, I., Morita, D., Hattori, Y., Kuwata, H., Fujiwara, N., Hiromatsu, K., Harashima, H., and Sugita, M. (2011) A microbial glycolipid functions as a new class of target antigen for delayed-type hypersensitivity. *J. Biol. Chem.* **286**, 16800–16806
76. Roura-Mir, C., Wang, L., Cheng, T. Y., Matsunaga, I., Dascher, C. C., Peng, S. L., Fenton, M. J., Kirschning, C., and Moody, D. B. (2005) *Mycobacterium tuberculosis* regulates CD1 antigen presentation pathways through TLR-2. *J. Immunol.* **175**, 1758–1766
77. Alibaud, L., Rombouts, Y., Trivelli, X., Burguière, A., Cirillo, S. L., Cirillo, J. D., Dubremetz, J. F., Guérardel, Y., Lutfalla, G., and Kremer, L. (2011) A *Mycobacterium marinum* *TesA* mutant defective for major cell wall-associated lipids is highly attenuated in *Dictyostelium discoideum* and zebrafish embryos. *Mol. Microbiol.* **80**, 919–934